Invariant line strain theory and its application to the crystallography of solid-state phase transformations*

LUO Chengping (罗承萍), XIAO Xiaoling (肖晓玲), LIU Jiangwen (刘江文) and WU Dongxiao (吴东晓)

(Department of Mechanical Engineering, South China University of Technology, Guangzhou 510641, China)

Received July 22, 1999; revised October 8, 1999

Abstract The formation mechanisms of the crystallographic features of phase transformation, including orientation relationship, habit plane, growth direction and transformation strain, are described; the early theoretical studies on the invariant line strain model are summarized; and the details of a "three-dimensional invariant line strain model" proposed by one of the authors and his colleague abroad are presented. The experimental results on the crystallographic features of needle-, rod- or lath-shaped precipitates formed in the FCC ⇔BCC and HCP ⇔BCC precipitation transformations were in excellent agreement with the predictions from the model, thus suggesting that the model could well serve as a phenomenological theory of crystallography for diffusion-controlled phase transformations.

Keywords: solid-state phase transformation, crystallographic feature, invariant line strain model, phenomenological theory.

The phenomenological theory of martensite crystallography (PTMC)[1—3] proposed in the early 1950's has been successfully employed to predict the crystallographic features of martensitic (shear) transformations, including the habit plane, orientation relationship (OR), the amount of lattice-invariant shear and the magnitude and direction of the shape deformation. However, no work was done on the crystallographic theory of diffusion-controlled (non-shear) transformations until the early 1980s when Dahmen and his co-workers[4,5] tackled this problem for the first time. Inspired by the conclusion that the crystallography of the martensitic transformations was determined by an "invariant plane strain" involved in the transformations, they proposed that the crystallography of a diffusion-controlled transformation might have been controlled by an "invariant line strain" associated with the transformation. By comparing the results of other investigators with the predictions from their won two-dimensional invariant line strain model, Dahmen et al.[4,5] confirmed the validity of the invariant line strain principle in explaining and predicting the crystallography of diffusion-controlled transformations. Immediately after Dahmen et al. proposed the model, Luo[1)], and Weatherly[6] extensively studied the theoretical aspects of the model, and precisely measured the crystallography of precipitation transformation in an Ni-Cr alloy, thus further confirming the effectiveness of the invariant line strain principle. A three-dimensional invariant line strain model[1),6] was then proposed, so that a more comprehensive crystallographic theory for diffusion-controlled phase transformations was developed. In this

* Project supported by the Research Fund for Doctoral Program of Higher Education (No. 98056111).

1) Luo, C. P., Ph. D. Dissertation: Crystalloraphy and interphase boundary structure of Cr-rich precipitates in a Ni-45wt% Cr alloy, University of Toronto, Toronto, 1986

review paper, the principle of the three-dimensional invariant line strain model is elucidated, the relevant calculational method is described, and the experimental results of crystallographic studies in some FCC/BCC and HCP/BCC alloy systems and their comparisons with theoretical predictions are presented.

1 Crystallography of phase transformation

The crystallographic features of a solid-state phase transformation usually include the orientation relationship between parent and product phases, habit plane, crystal growth direction, and the magnitude and direction of strain involved in the transformation; for a shear transformation, they include the relevant shear parameters in addition[3]. These features are thought to be attributed to the strain characteristic of the solid-state transformation.

The habit plane is an interface with a minimum interfacial energy, because both the chemical and structural components of the interfacial energy are usually minimum due to a good matching of the atoms in the two lattices across interface, and due to a small strain (dilatation and/or rotation) to which the habit plane is nominated during the transformation. According to the PTMC, the habit plane is an invariant plane in the parent phase that is neither rotated nor dilated in martensitic transformations. In a diffusion-controlled phase transformation like the precipitation transformation, however, the habit plane[6] is usually an "unrotated (untilted)" plane in the parent phase with small dilation. Meanwhile, it is a coherent or semicoherent interphase interface which has interfacial defects such as misfit dislocations and ledges. Since the interfacial misfit dislocations and ledges are generated to accommodate the misfit (strain) across the interface, the density of misfit dislocations and ledges in the low-energy habit plane must be low, thus making the habit plane a "clean interface", which has been repeatedly observed in precipitation transformations[7,8].

The orientation relationship is usually described with a pair of parallel lattice planes in the parent and product phases and a pair of parallel lattice directions lying in the common parallel planes. Sleeswyk[9], Ryder and Pitsch[10] independently studied the orientation relationship in phase transformation, finding that if a plane and a direction in the plane were assumed to keep unrotated (untilted) during the transformation, then the resultant orientation relationships could be described within a small region in a stereographic projection. As mentioned above, the unrotated plane is the possible habit plane of the transformation. It is therefore evident that the habit plane and orientation relationship can be simultaneously predicted based on the above assumption, and the invariant line strain model for predicting the crystallography of phase transformation was then proposed based on this assumption.

It has been observed that a needle-, rod-, or lath-shaped (Widdmannstatten) precipitate elongates (grows) in a specific high-index (irrational) lattice direction which is usually a few degs. (less than 10 degs.) apart from a close-packed direction in the parent phase (see refs. [6,11] for the lath-shaped precipitates). Theoretical analyses[4,5] and experimental studies[6,11] showed that this growth direction itself was the direction of the invariant line vector of the transformation. According to the definition of an invariant line, the misfit along the invariant line is zero, therefore a Widdmannstatten precipitate would naturally grow (elongate) parallel to the invariant line, so as to mini-

mize the strain free energy of the alloy system[5].

2 Invariant line strain models for solid-state phase transformations

2.1 Invariant line and invariant line strain

The invariant line strain can be derived from the invariant plane strain prevailing in the martensitic transformations. According to the PTMC[1—3], the martensitic transformation is accomplished via an invariant plane strain $\boldsymbol{P}_1$ consisted of three mathematical entities (strains): a lattice invariant shear (a simple shear) $\boldsymbol{P}$, a lattice deformation $\boldsymbol{B}$ and a rigid-body rotation $\boldsymbol{R}$:

$$\boldsymbol{P}_1 = \boldsymbol{RBP}. \tag{1}$$

Eq. (1) can be rewritten as

$$\boldsymbol{S} = \boldsymbol{P}_1\boldsymbol{P}^{-1} = \boldsymbol{RB}. \tag{2}$$

Since both $\boldsymbol{P}_1$ and $\boldsymbol{P}$ (and their inverses) are invariant plane strains, and the resultant of two invariant plane strains is an invariant line strain[3], $\boldsymbol{S} = \boldsymbol{RB}$ must be an homogeneous invariant line strain.

An invariant line is defined as a lattice direction vector in the parent phase, which is neither rotated nor extended (or contracted) by the phase transformation, thus becoming an intact direction in the product phase. Mathematically, an invariant line vector $\boldsymbol{X}_1$ possesses the following feature:

$$\boldsymbol{RBX}_1 = \boldsymbol{X}_1. \tag{3}$$

The lattice invariant shear $\boldsymbol{P}$ in eq. (1), and hence the invariant plane strain, are in general absent in a diffusion-controlled transformation, however, a rigid-body rotation of the product lattice relative to the parent one, $\boldsymbol{R}$, following the lattice deformation $\boldsymbol{B}$ is still needed to keep an optimum (energetically favoured) OR. The expression of the overall strain for a diffusion-controlled transformation is thus similar to that shown in eq. (2),

$$\boldsymbol{D} = \boldsymbol{RB}, \tag{4}$$

where $\boldsymbol{D}$ is the invariant line strain for a diffusion-controlled transformation; and it is obviously different from $\boldsymbol{S}$ in eq. (2), although both are referred to as invariant line strain.

2.2 Two-dimensional invariant line strain model

The process of the invariant line strain involved in a phase transformation can also be described figuratively with a circle-ellipse or sphere-ellipsoid analogue proposed by Bilby and Christian[12]. Fig. 1 shows a circle-ellipse analogue in which a circle with a unit radius (representing the parent phase) is transformed into an ellipse with axes a (< 1) and b (> 1) (representing the product phase) by a lattice deformation $\boldsymbol{B}$ (fig. 1(a)). There exists a specific vector $\boldsymbol{U}$ in the circle which, while keeping its magnitude unchanged, is rotated (tilted) by θ deg. By the lattice deformation, it becomes $\boldsymbol{BU}$. $\boldsymbol{U}$ is referred to as an unextended vector[4].

If a reverse rigid-body rotation θ is applied to vector $\boldsymbol{BU}$ to bring it back to its original position, $\boldsymbol{U}$ becomes an invariant line vector of phase transformation (fig. 1(b)). The final orientation relationship between the parent and product phases is therefore determined by the rigid-body rotation θ which, under a condition of invariant line strain, can be calculated in terms of the axes a and b[4],

$$\cos\theta = (1 + ab)/(a + b). \tag{5}$$

Figures 1(c) and (d) show an example of calculating the magnitudes of a and b and determining the final orientation relationship in terms of θ. If assuming the figure plane in figs. 1(c) and (d)

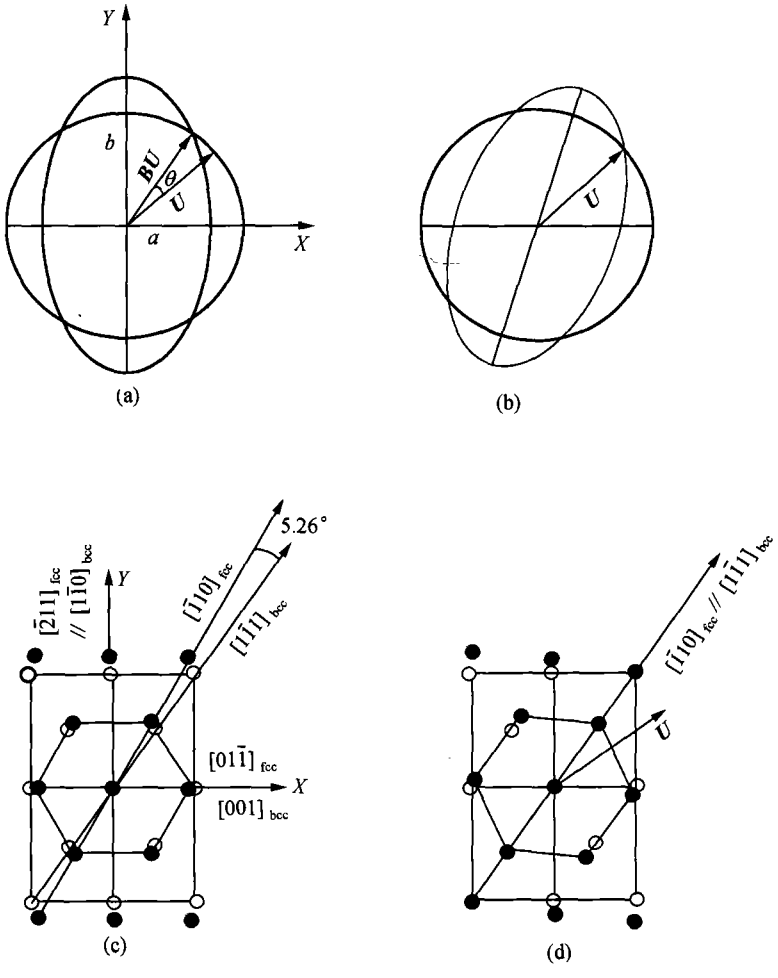

Fig. 1. A circle-ellipse analogue of solid-phase transformation. (a) A unit circle with radius of 1 is transformed into an ellipse with two axes a (< 1) and b (> 1) by the lattice distortion; (b) the vector $\boldsymbol{U}$ is transformed into an invariant line by rotating the ellipse (precipitate) θ deg. clockwise; (c) superposition of close-packed planes (111) of FCC lattice (full circles) and (110) of BCC lattice (open circles) in an N-W orientation relationship (corresponding to fig. 1 (a)); (d) rotating the FCC lattice 5.26 deg. Clockwise will lead to K-S orientation relationship (corresponding to fig. 1(b)).

to be parallel to the close-packed planes $(111)_f//(110)_b$ in an FCC/BCC system keeping an N-W orientation relationship described as $(111)_f//(110)_b$, $[01\bar{1}]_f//[001]_b$, $[\bar{2}11]_f//[1\bar{1}0]_b$(subscripts f and b stand for FCC and BCC lattices respectively) (fig. 1(c)), and setting up a coordinate system of

$$\boldsymbol{X}//1/2[01\bar{1}]_f \rightarrow [001]_b,$$

$$\boldsymbol{Y}//1/2[\bar{2}11]_f \rightarrow [1\bar{1}0]_b,$$

with the vector $1/2[01\bar{1}]_f$ transformed into $[001]_b$ along the $\boldsymbol{X}$ axis, and $1/2[\bar{2}11]_f$ into $[1\bar{1}0]_b$ along the $\boldsymbol{Y}$ axis, then a and b have the forms of

$$a = |[001]_b|/|1/2[01\bar{1}]_f| = a_b/((\sqrt{2}/2)a_f) = \sqrt{2}/(a_f/a_b),$$

$$b = |[1\bar{1}0]_b|/|1/2[\bar{2}11]_f| = 2\sqrt{2}a_b/(\sqrt{6}a_f = (2/3)/(a_f/a_b),$$

where a_f/a_b is the lattice parameter ratio of FCC to BCC lattices. When $a_f/a_b = \sqrt{2}$, for example, $a = 1$ and $b = \sqrt{6}$, and hence $\theta = 0°$ (eq. 5), indicating that no relative rotation takes place between the two lattices, thus keeping the N-W orientation relationship originally assumed in fig. 1(c) unchanged. If, on the other hand, $a_f/a_b = \sqrt{3}/\sqrt{2}$, then $\theta = 5.26°$, leading to a relative rotation of 5.26° between the two lattices, and hence to a K-S orientation relationship (fig. 1(d)). Accordingly, with a_f/a_b ranging from $\sqrt{3}/\sqrt{2}$ to $\sqrt{2}$, the orientation relationship will be located between K-S and N-W relationships. As shown in fig. 1(b), the relative rigid-body rotation will produce an invariant line $\boldsymbol{U}$ which is lying in the parallel close-packed planes $(111)_f//(110)_b$ and usually deviating by a small angle from the parallel close-packed direction $[\bar{1}10]_f//[1\bar{1}1]_b$(fig. 1(d)).

It is noted that the two-dimensional invariant line strain model proposed by Dahmen et al.[4,5] and discussed above assumes a pair of parallel close-packed planes in the two lattices, such as $\{111\}_f//\{110\}_b$ in FCC⇔BCC transformations and $(0001)_h//\{110\}_b$ in HCP⇔BCC transformations. Although this assumption is valid in a number of transformations, it restricts the flexibility of the invariant line strain model in predicting the crystallography of phase transformation. In addition, this model does not take into account the mathematical relation of the invariant line with the habit plane.

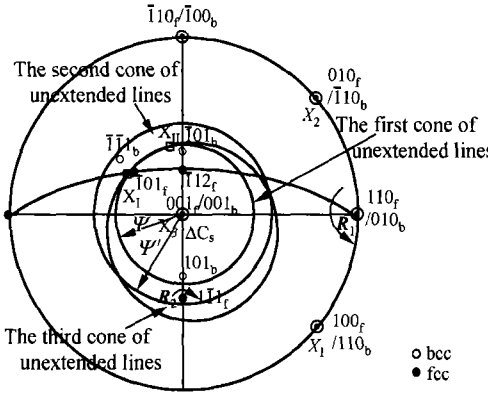

Fig. 2. A stereographic projection showing the Bain orientation relationship, the cones of unextended lines, and the scheme of determining the invariant line of phase transformation.

2.3 Three-dimensional invariant line strain model

If the vectors $\boldsymbol{U}$ and $\boldsymbol{BU}$ in fig. 1(a) are allowed to rigid-body rotate simultaneously around the $\boldsymbol{X}$ axis by 360 degs., then two coaxial cones with $\boldsymbol{U}$

and $\boldsymbol{BU}$ serving as their generatrices respectively are generated. The one formed by $\boldsymbol{U}$ is referred to as the first cone of unextended lines, and the one containing $\boldsymbol{BU}$ the second cone of unextended lines[3] (see fig. 2). By further rotating the second cone of unextended lines in such a manner that it intersects the first cone, two intersection lines are produced. According to the definition of the cone of unextended lines, the two intersection lines must be unextended but are not necessarily untilted. If the rotation itself can make one of the two intersection lines untilted at the same time, an invariant line vector results, and the transformation becomes invariant line strain controlled. The invariant line so formed is no longer necessarily lying in the close-packed planes, as with the case of the two-dimensional model. These rotation-intersection processes constitute the basis of calculating invariant line of phase transformation based on the three-dimensional invariant line strain model[6,11].

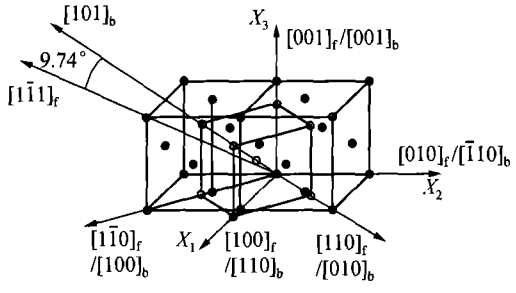

Fig. 3. A schematic diagram of Bain lattice distortion.

The concept of cone of unextended lines was first proposed to describe the Bain lattice deformation (fig. 3) involved in the FCC⇔BCC (BCT) transformations[3]. The Bain deformation is equivalent to an outward expansion by θ deg. of the first cone of unextended lines to reach the position of the second cone of unextended lines. The two cones can be described by equations consisted of the ratio a_f/a_b, and their semiapex angles relative to the $\boldsymbol{X}_3$ (contraction) axis of the Bain distortion, ψ and ψ' (fig. 2), are functions of the ratio a_f/a_b too[3]. Thus $\theta = \psi' - \psi$.

In order to calculate the invariant line and crystallography of a phase transformation, the strain matrix $\boldsymbol{D}$ in eq. (4) must be first calculated in terms of the Bain deformation $\boldsymbol{B}$ and rigid-body rotation $\boldsymbol{R}$. For the FCC⇔BCC(BCT) transformations, the Bain deformation is the most possible lattice deformation mode, because it involves the smallest possible atomic displacements[13]; the details of Bain deformation are shown in fig. 3. A BCT cell is delineated within the FCC lattice, and the Bain deformation is realized by compressing the BCT cell in the [001] direction and expanding it in [110] and $[\bar{1}10]$. As a result, a BCC cell is formed and a Bain orientation relationship produced (fig. 2). Based on the coordinate system in figs. 2 and 3, the matrix of the Bain deformation can be expressed as

$$\boldsymbol{B} = \begin{vmatrix} \eta_1 & 0 & 0 \\ 0 & \eta_2 & 0 \\ 0 & 0 & \eta_3 \end{vmatrix}, \tag{6}$$

where $\eta_1 = \eta_2 = \sqrt{2}/(a_f/a_b)$, and $\eta_3 = 1/(a_f/a_b)$. It should be noted that in other alloy systems involving crystal structure and correspondence other than the FCC/BCC ones, such as HCP/BCC, the pure lattice deformation affecting the structural change is also frequently referred to as the Bain deformation, or more specifically, the generalized Bain deformation[14].

The Bain deformation is usually followed by a rigid-body rotation of the product phase relative to its parent phase, so as to reach an energetically favoured orintation relationship or an optimum matching between the two phases. Mathematically, the rigid-body rotation may be realized either in a single step, or in several steps, depending on the range of the orientation relationship in consideration. The rotation matrix $\boldsymbol{R}$ in eq. (4) is then calculated in terms of the component rigid-body rotation(s). For example, the K-S orientation relationship can be reached in two steps (fig. 2). Specifically, starting from the Bain OR, a rotation $\boldsymbol{R}_1(\theta_1) = 9.74°/[110]_f$ will result in an N-W OR, and a further rotation from the N-W OR, $\boldsymbol{R}_2(\theta_2) = -5.26°/[1\bar{1}1]_f$ leads to a K-S OR. The total rigid-body rotation for obtaining the K-S OR is therefore $\boldsymbol{R} = \boldsymbol{R}_2\boldsymbol{R}_1$. A right-hand rule is used to define the sense of the rotation angle: a clockwise rotation giving a negative angle, while a counterclockwise rotation a positive one. The K-S OR resulting from the above rotations are described as

$$\begin{aligned} &(1\bar{1}1)_f//(101)_b, \\ &[\bar{1}01]_f//[\bar{1}\,\bar{1}1]_b, \\ &[\bar{1}21]_f//[121]_b. \end{aligned} \tag{7}$$

It is seen from fig. 2 that the second cone of unextended lines is rotated by $\boldsymbol{R}$, reaching a new position and becoming the third cone of unextended lines or the rotated second cone. The third cone of unextended lines intersects the first cone at $\boldsymbol{X}_{\mathrm{I}}$ and $\boldsymbol{X}_{\mathrm{II}}$, producing two intersection lines $\boldsymbol{X}_{\mathrm{I}}$ and $\boldsymbol{X}_{\mathrm{II}}$, one of which (assumed to be $\boldsymbol{X}_{\mathrm{I}}$) is the possible invariant line of the transformation.

2.4 Calculation of the invariant line

The indices of the intersection lines $\boldsymbol{X}_{\mathrm{I}}$ and $\boldsymbol{X}_{\mathrm{II}}$ can be calculated using matrix algebraic method based on a scheme illustrated in fig. 2. The readers may refer to refs. [6,11] for details of the calculation. According to the definitions of the cones of unextended lines, $\boldsymbol{X}_{\mathrm{I}}$ and $\boldsymbol{X}_{\mathrm{II}}$ so obtained are all unextended, but not necessarily all invariant. If $\boldsymbol{RBX}_i = \boldsymbol{X}_i$, then $\boldsymbol{X}_i$ is an invariant line. The geometry in fig. 2 dictates that only $\boldsymbol{X}_{\mathrm{I}}$ can be an invariant line.

If a given rotation $\boldsymbol{R}$ equivalent to a measured or assumed OR is used in the calculation, then the resultant $\boldsymbol{X}_{\mathrm{I}}$ may not be but very close to a genuine invariant line[6]. In order to obtain a genuine invariant line, and hence to ensure a genuine invariant line strain, the OR should not be fixed beforehand in the calculation. Instead, it should be determined based on a first principle of invariant line strain[4]. In the calculation illustrated in fig. 2, for example, only the first rotation is fixed at $\boldsymbol{R}_1(\theta_1) = 9.74°/[110]_f$, while $\boldsymbol{R}_2(\theta_2) = \theta_2/[1\bar{1}1]_f$ is allowed to vary to produce an invariant line. Obviously, the first rotation leads to a relationship $(1\bar{1}1)_f//(101)_b$ (eq. (7)). A searching and finding computer program was worked out and used to calculate the invariant line $\boldsymbol{X}_{\mathrm{I}}$ and the accompanying rotation angle θ_2. In the present calculation, $\boldsymbol{X}_{\mathrm{I}}$ is taken to be a genuine invariant line if the angle between $\boldsymbol{RBX}_{\mathrm{I}}$ and $\boldsymbol{X}_{\mathrm{I}}$ is equal to or less than 0.0001°. The calculations showed that θ_2 for producing an invariant line was slightly ($< 0.5°$) deviating from that in an FCC/BCC alloy system with a lattice parameter ratio around 1.25, suggesting that the OR for which a genuine invariant line strain

occurred should be in fact not a genuine K-S one. In this case, the close-packed directions in the two phases, $[\bar{1}01]_f$ and $[\bar{1}\,\bar{1}1]_b$, (eq. (7)) were slightly apart, which could be most clearly shown and measured in the composite electron diffraction pattern $[1\bar{1}1]_f//[101]_b$[6,11].

According to the principle of matrix algebra, the invariant line and unextended lines (vectors) associated with the transformation should be equivalent to the eigenvectors $\boldsymbol{V}_1$, $\boldsymbol{V}_2$ and $\boldsymbol{V}_3$ which are in turn determined by the eigenvalues λ_1, λ_2 and λ_3 of the invariant line strain $\boldsymbol{RB}$. An eigenvector is actually an untilted line vector. It is also pointed out[3,12] that the magnitudes of the three principal strains of $\boldsymbol{RB}$ are λ_1, λ_2 and λ_3, and their directions parallel to $\boldsymbol{V}_1$, $\boldsymbol{V}_2$ and $\boldsymbol{V}_3$ respectively. (The three principal strains so determined are no longer orthogonal.) For an invariant line strain, one of the three eigenvalues (assumed to be λ_1) must be equal to unity, and the other two greater and less than unity respectively[12]. $\boldsymbol{V}_1$ is therefore an invariant line and the others are merely untilted lines. Calculation[11] showed that $\boldsymbol{V}_1$ and $\boldsymbol{X}_1$ were indeed identical.

2.5 Crystallographic predictions based on the invariant line strain model

It is evident from the above discussions that the Bain deformation followed by the relative rigid-body rotation(s) dictated by an invariant line strain yields an OR of the transformation. In the calculation represented in fig. 2, $\boldsymbol{R}_1(\theta_1) = 9.74°/[110]_f$ is first given, while θ_2 in $\boldsymbol{R}_2(\theta_2) = \theta_2/[1\bar{1}1]_f$ is allowed to vary to produce an invariant line. The final OR of the transformation can therefore be precisely predicted by the invariant line strain model, if a range of the OR such as that dictated by $\boldsymbol{R}_1(\theta_1)$ is known or given. It should be noted that the assumption of $\boldsymbol{R}_1(\theta_1) = 9.74°/[110]_f$ restricts the generality of crystallographic calculations, though it is valid in a number of precipitation transformations having parallel close-packed planes (see table 1), and it can make the calculations simpler.

Table 1 A comparison of the calculated and experimental crystallographic features for three diffusional precipitation transformations

Alloy and transformation	Crystallographic features	Experimental	Calculated	Discrepance
Cu-0.33wt.% Cr[11]	habit plane	$(3.1,3.5,5.5)_{fcc}$;	$(3.45,3.10,5.19)_{fcc}$;	1.4°
(FCC→BCC)	growth	$[\bar{5},6,\bar{1}]_{fcc}$;	$[\bar{0.63},0.76,\bar{0.13}]_{fcc}$;	0.1°
Diffusional	direction	$(111)_{fcc}//(110)_{bcc}$;	$(111)_{fcc}//(110)_{bcc}$;	0°
transformation	OR	$[\bar{1}10]_{fcc}+0.5°\rightarrow[1\bar{1}1]_{bcc}$	$[\bar{1}10]_{fcc}+0.5°\rightarrow[1\bar{1}1]_{bcc}$	
		$[11\bar{2}]_{fcc}+0.5°\rightarrow[\bar{1}12]_{bcc}$	$[11\bar{2}]_{fcc}+0.5°\rightarrow[\bar{1}12]_{bcc}$	
Cr-10wt.% Ni[17]	habit plane	$(1,2,1)_{fcc}$;	$(0.427,0.813,0.395)_{fcc}$;	0.2°
(BCC→FCC)	growth	$[\bar{12},1,11]_{fcc}$;	$[\bar{0.733},0.056,0.677]_{fcc}$;	0.4°
Diffusional	direction	$(111)_{fcc}//(101)_{bcc}$;	$(111)_{fcc}//(110)_{bcc}$;	
transformation	OR	$[\bar{1}01]_{fcc}+0.33°\rightarrow[\bar{1}\,\bar{1}1]_{bcc}$	$[\bar{1}01]_{fcc}+0.3°\rightarrow[\bar{1}\bar{1}1]_{bcc}$	0.03°
		$[\bar{1}2\bar{1}]_{fcc}+0.33°\rightarrow[\bar{1}21]_{bcc}$	$[\bar{1}2\bar{1}]_{fcc}+0.3°\rightarrow[\bar{1}21]_{bcc}$	
Zr-2.5wt.% Nb[15]	habit plane	$(0001)_{hcp}//(110)_{bcc}$	$(0001)_{hcp}//(110)_{bcc}$	0°
(HCP→BCC)	growth	$6.4°\rightarrow[10\bar{1}0]_{hcp}$	$8.2°\rightarrow[10\bar{1}0]_{hcp}$	1.8°
Diffusional	direction	in plane$(0001)_{hcp}$	in plane$(0001)_{hcp}$	
transformation	OR	$(0001)_{hcp}//(110)_{bcc}$	$(0001)_{hcp}//(110)_{bcc}$	
		$[11\bar{2}0]_{hcp}+1.5°\rightarrow[1\bar{1}1]_{bcc}$	$[11\bar{2}0]_{hcp}+1.3°\rightarrow[1\bar{1}1]_{bcc}$	0.2°
		$[1\bar{1}00]_{hcp}+1.5°\rightarrow[\bar{1}12]_{bcc}$	$[1\bar{1}00]_{hcp}+1.3°\rightarrow[\bar{1}12]_{bcc}$	

Since there is no misfit between the two lattices along an invariant line, a needle-, rod- or lath-

shaped precipitate would naturally grow along this line, so as to lower the strain energy incurred by the transformation[5]. Dahmen[4] has indicated that an invariant line has zero directional misfit in the real space, and is perpendicular to the direction with minimum planar mismatch in the reciprocal space. In other words, the invariant line is lying in a set of parallel and minimum-mismatched planes in the two lattices. In the FCC/BCC or HCP/BCC systems, for example, the invariant line of transformation is usually lying in the parallel or nearly parallel close-packed planes $\{111\}_f/\{110\}_b$ or $(0001)_h/\{110\}_b$(table 1).

Being an interface with minimum misfit (strain), the habit plane is defined by the invariant line and an untilted line in the present invariant line strain model[6,12]. It can therefore be determined by $V_1 \times V_2$ or $V_1 \times V_3$. The habit plane so determined is obviously an untilted plane.

Each two of the three eigenvectors (untilted vectors) V_1, V_2 and V_3 can be cross-multiplied to define a plane, hence the three planes so determined are all untilted and may serve as a habit plane or interface. The interfaces (habit plane) containing the invariant line, namely $V_1 \times V_2$ and $V_1 \times V_3$ have, whereas the one not containing the invariant line, viz. $V_2 \times V_3$ has not, been observed in lath-shaped precipitates[11,17]. Which of the interfaces $V_1 \times V_2$ and $V_1 \times V_3$ is taken to be the habit plane is judged based on (i) the magnitudes of V_2 and V_3, and (ii) the density of interfacial defects such as dislocations and ledges in the interface. An interface defined by V_1 and the smaller V_2 and V_3, and/or having a minimum defect density is likely to be the habit plane. The interfacial dislocations and ledges are formed to accommodate the misfits across the interface, so that the habit plane with minimum misfit would contain a minimum density of defects, thus manifesting itself as a "clean interface"[7,8].

As with the PTMC, the invariant line strain model provides merely a phenomenological description of the transformation crystallography, saying nothing about the mechanism of atomic displacements involved in the transformation. While the PTMC is proposed for a shear transformation, the invariant line strain model is developed for a diffusion-controlled one, thus it can be referred to as a phenomenological theory of diffusional transformation crystallography.

3 Comparisons of the predicted and experimental crystallographies

The theoretical and experimental studies of crystallography of phase transformations based on the invariant line strain model have so far essentially focused on the FCC⇔BCC transformations, although some preliminary studies on the HCP⇔BCC ones have been conducted[15,16]. Listed in table1 are the experimental crystallographic features (OR, habit plane and growth direction) and their comparisons with the predictions from the invariant line strain model for the precipitation reactions occurring in Cu-Cr(FCC→BCC)[11], Cr-Ni(BCC→FCC)[17] and Zr-Nb(HCP→BCC)[15]. In order to enhance the accuracy of the experimental measurements, special TEM methods developed by the authors in their prolonged crystallography studies of phase transformations, including the double edge-on trace analysis for habit plane (interface) orientation measurement[18], making use of special (low-index) composite electron diffraction patterns for OR determination[6,11], and oriented-tilt trace analysis for determining the growth (axial) direction of Widdmannstatten precipitates[11], have been utilized to gather the

crystallographic information of these transformations.

It is evident from table1 that the experimental crystallographic features of the three precipitation transformations are in excellent agreement with those predicted by the invariant line strain model, thus suggesting that the model is valid in predicting the crystallography of diffusional Widdmannstatten precipitation. It should be noted that not only the $V_1 \times V_2$ habit planes of $\{335\}_f$ in Cu-Cr[11] and $\{112\}_f$ in Ni-Cr[6] and Cr-Ni[17], but also the $V_1 \times V_3$ interfaces which were found to be the parallel planes $\{111\}_f/\{110\}_b$ in all these alloy systems, were experimentally observed. As predicted, all these interfaces contain the invariant line. The $\{335\}_f$ and $\{112\}_f$ were considered as the habit planes, because they met the two conditions for a habit plane: (i) being defined by the invariant line V_1 and the smaller (contracted) untilted V_2, and (ii) being a "clean interface" containing minimum ledge density in it.

4 Summary

(i) A lattice direction vector in the parent lattice, which is neither rotated nor extended (or contracted) by the transformation strain, thus becoming an intact direction vector in the product lattice, is referred to as an invariant line of the transformation; and the transformation strain needed to produce the invariant line is referred to as the invariant line strain. There is no misfit between the two lattices along the invariant line.

(ii) The morphology of needle-, rod- or lath-shaped precipitates produced in diffusional precipitation transformations is controlled by the invariant line strain; these precipitates grow parallel to the invariant line vector, with their side interfaces (if any), including the habit plane containing the invariant line.

(iii) Mathematically, the invariant line strain consists of the pure lattice deformation $\boldsymbol{B}$ and the rigid-body rotation $\boldsymbol{R}$ of the product lattice relative to the parent lattice. The classic Bain deformation is thought to be responsible for the lattice deformation in the FCC⇔BCC(BCT) transformations; whereas a generalized Bain deformation which, like the classic one, involves the smallest possible atomic displacements, serves as the mode of lattice deformation in other transformations such as HCP⇔BCC.

(iv) Using the matrix algebraic method and a searching and finding computer program, the invariant line vector and the untilted vectors of a transformation, or the eigenvectors of the invariant line strain $\boldsymbol{RB}$, the magnitude and sense of the rigid-body rotation(s) between the two lattices, and the invariant line strain matrix involved in the transformation can be calculated in terms of the lattice parameters of the two lattices, and of the modes of the Bain deformation and rigid-body rotation.

(v) The crystallographic features of a transformation can be predicted based on the calculations given in (iv) as follows. A needle-, rod-, or lath-shaped precipitate is assumed to grow (elongate) along the invariant line. The OR between the two lattices is determined by the Bain deformation followed by the rigid-body rotation(s). The untilted habit plane and other interfaces are defined by the invariant line and an untilted line.

(vi) The experimental crystallographic features of the FCC⇔BCC transformations in Cu-Cr and Cr-Ni alloys, as well as those of the HCP⇔BCC one in Zr-Nb alloy are in excellent agreement with those predictions based on the invariant line strain model, thus suggesting that the model is valid for predicting the crystallography of diffusional precipitations producing Widdmannstatten precipitates and can well serve as a phenomenological theory of diffusional transformation crystallography.

References

1 Wecshsler, M. S., Lieberman, D. S., Read, T. A., On the theory of the formation of martensite, *Trans. Am. Ins. Min. Engrs.*, 1953, 197: 1503.

2 Bowles, J. S., Mackenzie, J. K., The crystallography of martensite transformation, *Acta Metall.*, 1954, 2: 129.

3 Wayman, C. M., *Introduction to the Crystallography of Martensitic Transformations*, New York: MacMillan, 1964.

4 Dahmen, U., Orientation relationships in precipitation systems, *Acta Metall.*, 1982, 30: 63.

5 Dahmen, U., Ferguson, P., Westmacott, K. H., Invariant line strain and needle-shaped precipitate growth direction in Fe-Cu, *Acta Metall.*, 1984, 32: 803.

6 Luo, C. P., Weatherly, G. C., The invariant line and precipitation in a Ni-45wt.%Cr alloy, *Acta Metall.*, 1987, 35: 1963.

7 Luo, C. P., Weatherly, G. C., The interphase boundary structure in a Ni-Cr alloy, *Philos. Mag.*, 1988, A58: 445.

8 Luo, C. P., Dahmen, U., Interface structure of faceted lath-shaped precipitates in a Cu-0.33wt.%Cr alloy, *Acta Mater.*, 1998, 46: 2063.

9 Sleeswyk, A. W., The crystallography of the austenite-cementite transition, *Philos. Mag.*, 1966, A13: 1223.

10 Ryder, P. L., Pitsch, W., The crystallography analysis of grain boundary precipitation, *Acta Metall.*, 1966, 14: 1437.

11 Luo, C. P., Dahmen, U., Westmacott, K. H., Morphology and crystallography of Cr-precipitates in a Cu-0.33wt.%Cr alloy, *Acta Metall. Mater.*, 1994, 42: 1923.

12 Bilby, B. A., Christian, J. W., Martensitic transformations, in *The Mechanism of Phase Transformations in Metals*, Institute of Metals, Monograph and Report Series No. 18, London, 1956, 121.

13 Jawson, M. A., Wheeler, J. A., Atomic displacement in the austenite-martensite transformation, *Acta Crystallogr.*, 1948, 1: 216.

14 Wayman, C. M., The phenomenological theory of martensite crystallography: interrelationship, *Metall. Trans.*, 1994, 25A: 1787.

15 Luo, C. P., Weatherly, G. C., The precipitation behaviour of a Zr-2.5wt.%Nb alloy, *Metall. Trans.*, 1988, 19A: 1153.

16 Lang, J. M., Dahmen, U., Westmacott, K. H., The origin of Mo_2C precipitate morphology in molybenum, *Phys. Stat. Sol.*(a), 1983, 75: 409.

17 Luo, C. P., Wu, D. X., Xiao, X. L., Crystallography of the BCC⇔FCC transformation in a Cr-10wt.%Ni alloy, *Abstract (Letters) of Science and Technology of China* (in Chinese), 1996, 2(10): 121.

18 Luo, C. P., Xiao, X. L., Wu, D. X., A TEM method for accurate measurement of habit plane (interface): double edge-on trace analysis, *Progress in Natural Science*, 1997, 7(6): 742.